International Journal of Thermal Sciences 109 (2016) 33–43

Contents lists available at ScienceDirect

International Journal of Thermal Sciences

journal homepage: www.elsevier.com/locate/ijts

The isokinetic behavior in diffusion controlled growth processes

M. Fontana [a, *], M.A. Ureña [a], B. Arcondo [a], M.T. Clavaguera-Mora [b]

[a] Laboratorio de Sólidos Amorfos, INTECIN, Facultad de Ingeniería, Universidad de Buenos Aires – CONICET, Paseo Colon 850, 1063 Buenos Aires, Argentina
[b] Grup de Nanomaterials i Microsistemes, Departament de Física, Universitat Autònoma de Barcelona, Edifici C, 08193 Bellaterra, Spain

ARTICLE INFO

Article history:
Received 4 January 2016
Received in revised form
19 May 2016
Accepted 19 May 2016

ABSTRACT

The isokinetic behaviour of crystallization processes controlled by diffusion is analysed under both isothermal and continuous cooling/heating conditions. The kinetic function is computed employing an approximate expression for the so called exponential integral. Diffusion controlled 3D growth of homogeneously nucleating crystalline grains is an isokinetic reaction if the nucleation and diffusion activation energies are identical. In the non isokinetic range, the kinetic functions in both continuous heating and isothermal transformations are the same except for a factor which depends on the nucleation and diffusion activation energies ratio. This development is applied to the crystallization of AgGeSe glasses. The primary crystallization kinetic of glasses with compositions $(Ge_{25}Se_{75})_{100-y}$ Ag_y (with y = 10, 15, 20 and 25 at. %) was studied in a previous work using differential scanning calorimetry and X-ray diffraction. The analysis is grounded on the Kolmogorov-Johnson-Mehl-Avrami model generalized to account for the compositional changes of the parent phase, responsible for the decreasing of both the nucleation frequency and the growth rate of the primary grains. The kinetic study of the crystallization process from continuous heating calorimetric data has been performed applying the *master curve method*. The primary crystallization product is the ternary phase γ-Ag_8GeSe_6. The values of apparent activation energy E_a, obtained are in the range: 2.0 eV/at < E_a < 2.6 eV/at. A model of diffusion controlled 3D growth with decreasing homogeneous nucleation and soft impingement has been developed that reproduces the rate of transformation obtained experimentally for the studied alloys.

1. Introduction

The knowledge of the crystallization kinetics is a key point in order to design controlled procedures for the improvement of the properties that depend on the microstructure. Nowadays, the transformation kinetics is considered as a very essential subject, which gives information relative to the stability and thus the applicability of the materials. This topic is a permanent reason of analysis and it is currently studied in many works [1–13]. Therefore, the knowledge of the mechanisms affecting the transformation kinetics is a key point. In particular, it is interesting the use of simple kinetic models based on average behaviours using only a few parameters. The development of the classical crystallization model (Kolmogorov-Johnson-Mehl-Avrami (JMAK) theory) [14–20] is based on laws of nucleation and growth. In the growth of a precipitate in a supersaturated liquid, two different growth habits that can be actually superimposed in real processes are distinguished [9]:

a) When the compositions of both the emerging crystalline and the remaining non-transformed phases are identical, the precipitated nucleus grows radially with a constant growing rate, under isothermal conditions. The nucleus grows until impingement with other nuclei stops growing.
b) When a crystalline phase of different composition than the remaining liquid precipitates, as in primary crystallization, an interface between the crystal and liquid exists where a concentration gradient of solutes acts as a resistance to the flow of both the solute atoms towards the crystalline nucleus and of the atoms rejected from the crystalline nucleus. The growth process is controlled by diffusion.

On the other hand, the “additivity rule” has been used to predict the kinetics of transformation under non-isothermal conditions [2–8,14,15]. The conventional hypothesis for additivity is that the transformation behaviour during continuous cooling/heating can be described as the overlap of isothermal transformations with very short periods of time. Christian [14] proposed a sufficient condition

* Corresponding author.
E-mail address: mfontan2006@gmail.com (M. Fontana).

http://dx.doi.org/10.1016/j.ijthermalsci.2016.05.020
1290-0729/

for the additivity rule: the transformation rate dx/dt is a separable function of the temperature T and transformed fraction x that is:

$$\frac{dx}{dt} = \frac{h(T)}{P(x)} \tag{1}$$

where $h(T)$ is the rate constant and $P(x)$ the kinetic function.

The validity of the classic additivity rule was recently studied for diffusional growth [6] and the KJMA model [7, 10] under lineal temperature variation. Based on the exact solution of non-isothermal diffusion controlled growth, a generalized additivity rule compatible with the thermal history was proposed [6]. In the framework of the JMAK theory and using also an exact calculation [10], it is demonstrated that dx/dt separates in a product as Eq. (1).

In the present work, the kinetic study of the crystallization process of glasses in the system GeSeAg from continuous heating calorimetric data has been performed applying a recently developed procedure: the master curve [21–23]. A brief summary of this method is included in Section 1. This procedure is valid if the crystallization processes are isokinetic [21–23]. A process can be defined as isokinetic if the kinetic function $P(x)$ is the same under both isothermal and continuous cooling/heating conditions. It is also called isokinetic range [7, 14, 15]. The validation of the isokinetic process hypothesis in the case of 3D growth controlled by interface has been developed [23] and a summary of the theory of the growth controlled by interface is shown in Appendix A.

The crystallization mode in glasses is in general a primary crystallization of a new phase with a composition that differs from the parent phase. Therefore, the diffusion is the mechanism that governs the crystallization. This is the case of the crystallization of GeSeAg glasses. In the present work, the validation of this isokinetic hypothesis in the case of diffusion controlled three-dimensional growth is analysed and introduced in the Section 2 and Appendix B. The kinetic function $P(x)$ is computed employing an approximate expression of the so called temperature integral (in the case of large activation energy) [7]. Others authors [2–4, 7, 8, 11] performed similar procedures for the interphase and/or diffusion controlled growth. However, a novel analysis of the kinetic function is shown in the Section 2 and Appendix B: in the non-isokinetic range, $P(x)$ is the same function in both continuous heating and isothermal conditions except for a factor $\Psi_{5/2}$ which depends on the nucleation and diffusion activation energies ratio.

The application of this procedure to the crystallization of AgGeSe amorphous alloys is shown in Section 3. The analysis of the kinetic mechanisms involved in the crystallization process of AgGeSe glasses is introduced in Section 3.2. A model of diffusion-controlled-3D growth with decreasing homogeneous nucleation and soft impingement has been developed. Conclusions are shown in 4.

1.1. New approach for kinetic analysis: master curve analysis of a transformation in continuous heating regimes

The "master curve method" was introduced in recent works [21–23]. Kinetic analysis of solid state reactions are usually performed by considering that transformation rate can be expressed in terms of a first-order separable differential equation. Under isothermal annealing at temperature T, imposing an Arrhenian temperature dependence for both nucleation and growth rate, dx/dt may be expressed as [21–24].

$$\frac{dx}{dt} = \frac{\exp\left(\frac{-E_a}{kT}\right)}{P_{iso}(x)} \tag{2a}$$

where x is the scaled transformed volume fraction of the primary phase, E_a is the apparent activation energy, k is the Boltzmann's constant and $P_{iso}(x)$ a kinetic function dependent on the transformation mechanisms.

Under continuous heating at a constant rate $\beta = dT/dt$, the equivalent form of Eq. (2a) gives the transformation rate dx/dT as

$$\frac{dx}{dT} = \frac{\exp\left(\frac{-E_a}{kT}\right)}{\beta P_{HR}(x)} \tag{2b}$$

where $P_{HR}(x)$ is the continuous heating counterpart of $P_{iso}(x)$.

In Eqs. (2a) and (2b), the apparent activation energy in both transformation types (isothermal and continuous heating regimes) is supposed to be constant. In general, this hypothesis is valid in a limited temperature interval (for example, in the range of calorimeter experimental measurements).

Eqs. (2a) and (2b) verify the additivity rule and they are particular cases of the Eq. (1) (the separable differential equation for the transformation rate [14]).

The master curve method relies on the validity of Eq. (2b) for the transformation rate under continuous heating at a constant rate β. Since it is a first order separate differential equation, it can be integrated as follows:

$$\int_0^x P_{HR}(x)dx = \frac{\int_{To}^{T} \exp\left(\frac{-E_a}{kT}\right)dT}{\beta} \tag{3}$$

where T_o is the onset temperature, T_o and T are those measured at the heating rate.

The integral on the right-hand side is independent of thermal history and depends only on the evolution of x, involving the transformation mechanisms. So, for different heating rates, β and β' it can be written:

$$\int_0^x P_{HR}(x)dx = \frac{\int_{To}^{T} \exp\left(\frac{-E_a}{kT}\right)dT}{\beta} = \frac{\int_{To}^{T'} \exp\left(\frac{-E_a}{kT}\right)dT}{\beta'} = \frac{\int_{To}^{Teq} \exp\left(\frac{-E_a}{kT}\right)dT}{\beta_{eq}} \tag{4a}$$

where it can be generalized for an equivalent heating rate β_{eq} and an equivalent temperature T_{eq}.

Further, if $E/RT >> 1$, the right term of Eq. (4a) can be written as (See Eq. (B-2) in Appendix B):

$$\frac{T^2}{\beta}\exp\left(\frac{-E_a}{kT}\right) = \frac{T_{eq}^2}{\beta_{eq}}\exp\left(\frac{-E_a}{kT_{eq}}\right) \tag{4b}$$

This assumption $E/RT >> 1$ is reasonable because $15 < E/RT < 60$ is valid for the vast majority of solid-state reactions [28,29].

In the temperature range where the transformation occurs Eq. (4b) can be used for the set of continuous heating DSC data (curves $\{dx/dT_i, T_i\}$) obtained at heating rate β_i with $(i = 1,\ldots,p)$, to convert them to a single curve $\{dx/dT_{eq}, T_{eq}\}$ at the equivalent heating rate β_{eq}. The activation energy is obtained by analysing the overlap of the different curves.

The conversion method is established iteratively:

a. An initial activation energy E_a is determined (for instance, by the Kissinger plot [16]) and Eq. (4b) is used to obtain T_{eq}, i.e., for each set $\{T_i(dx/dT_i), \beta_I\}$, the equivalent set $\{T_{eq}(dx/dT_i), \beta_{eq}\}$.

b. Integration of dx/dT_i with respect to the converted temperature T_{eq} in the overall transformation range (from the start T^{onset} to the end point T^{end}) gives the weighted factor, $C(\beta_I, \beta_{eq})$, needed to transform dx/dT_i to dx/dT_{eq}:

$$\frac{dx}{dT_{eq}} = \frac{\frac{dx}{dT}}{C\left(\beta, \beta_{eq}\right)} \quad with\ C\left(\beta, \beta_{eq}\right) = \int_{Tonset}^{Tend} \frac{dx}{dT} dT_{eq} \tag{5}$$

since

$$\int_{T^{onset}}^{T^{end}} \frac{dx}{dT_{eq}} dT_{eq} = 1$$

c. A new activation energy E_a is estimated by minimising the differences between the various sets $\{dx/dT_{eq}, T_{eq}\}$ obtained from each set of continuous heating DSC curves $\{dx/dT_i, T_i\}$ at heating rate β_I.
d. Steps (b) and (c) are repeated until the differences between the various sets $\{dx/dT_{eq}, T_{eq}\}$ of two subsequent iteration steps are negligibly small.

This method provides a more accurate determination of E_a than the procedures based on the peak temperature of the DSC curves. The activation energy determined by this method is a "weighted" average in the limited temperature range where measurements were made.

Furthermore, it provides a calorimetric curve, the master curve (T_{eq}, dx/dT_{eq}) for the given heating rate β_{eq}. This master curve is the average of all the experimental continuous heating scans. It has a better signal/noise ratio than the individual curves. The knowledge of this master curve determines experimentally the function $P_{HR}(x)$ using Eq. (2b):

$$P_{HR}(x) = \frac{\exp\left(\frac{-E_a}{kT_{eq}}\right)}{\beta_{eq}\frac{dx}{dT_{eq}}} \tag{6}$$

1.2. Johnson-Mehl-Avrami-Kolmogorov theory

Most often, the kinetic analysis of non-isothermal transformation assumes the KJMA model. The knowledge of the kinetic model allows determine $P_{iso}(x)$ or $P_{HR}(x)$ in Eqs. (2a) and (2b). In general, under isothermal conditions, the kinetic function $P_{iso}(x)$ in the KJMA model is written as [9,14,23,24]:

$$P_{iso}^{KJMA}(x) = \frac{P_{0,iso}[-\ln(1-x)]^{\frac{1-n}{n}}}{n(1-x)} \tag{7}$$

where n is called Avrami exponent and $P_{0,iso}$ is a constant factor.

It is useful to know the integral function of $P_{iso}^{KJMA}(x)$:

$$G_{iso}^{KJMA}(x) = \int_0^x P_{iso}^{KJMA}(x)dx = P_{o,iso}[-\ln(1-x)]^{1/n} \tag{8}$$

In a previous work [23], a KJMA model with homogenous and constant nucleation and three-dimensional *interface-controlled growth* was elaborated under isothermal and continuous heating regimes. A summary of the theory of the *growth controlled by interface* is shown in Appendix A. It uses the following hypothesis:

a) The nucleation critical radius is negligible.
b) An Arrhenian temperature dependence for both nucleation frequency I(T) and growth rate u(T), that is:

$$I(T) = I_o \exp\left(\frac{-E_I}{kT}\right) \tag{9a}$$

$$u(T) = u_o \exp\left(\frac{-E_U}{kT}\right) \tag{9b}$$

where E_I, and E_U are the activation energies for nucleation and growth, respectively, and I_o and u_o the pre-exponential factors.

This analysis developed in Ref. [23] and Appendix A for the *interface controlled growth processes*, has not been done yet for diffusion controlled growth processes. Therefore, one of the main purposes in this work is to analyse if relations similar to Eqs. (A-3) and (A-4) of the Appendix A exist for homogeneous nucleation and 3D diffusion-controlled growth transformations. This development is introduced in the Section 2.

2. Johnson-Mehl-Avrami-Kolmogorov theory. Growth controlled by diffusion

The experimental study of the transformation kinetics in amorphous materials is mainly based on calorimetric analysis, so it would be desirable to predict the calorimetric signal by a theoretical approach based on the nucleation and growth mechanisms.

Since the calorimetric signal is proportional to dx/dt, it can be deduced from the JMAK theory [14–20]. In this framework an extended volume is defined, where the grains can grow freely without geometrical impediment, and the extended transformation fraction, x_{ex}, is related to the real one, x, by Ref. [14]:

$$x = 1 - \exp(-x_{ex}) \tag{10}$$

In this way the transformed fraction can be obtained based only on the transformation mechanisms of nucleation and growth. In the case of a transformation with a homogeneous nucleation frequency, I, the extended transformation fraction can be written as:

$$x_{ex} = \int_0^t I v(\tau) d\tau \tag{11}$$

where $v(\tau)$ is the volume of a grain nucleated at the instant τ.

For a three-dimensional growth controlled by diffusion with an initial nucleation critical radius r^*, the volume $v(\tau)$ is:

$$v(\tau) = \frac{4\pi}{3}\left[r^{*2} + \int_\tau^t D dt'\right]^{3/2} \tag{12}$$

With D the diffusion coefficient.

When a broad range of temperature is considered, the temperature dependence of nucleation frequency and diffusion coefficient are far from an Arrhenian type. However, over a limited range of temperature (as it is the case of crystallization peaks in DSC experiments) $I(T)$ and $D(T)$ may be described approximately by an Arrhenius expression, that is Eq. (9a) for $I(T)$ and:

$$D(T) = D_o \exp\left(\frac{-E_D}{kT}\right) \tag{13}$$

where D_o is the pre-exponential factor and E_D the activation energy for the diffusion.

2.1. Isothermal regime

Therefore, the extended transformation fraction x_{ex} as a function of time at a constant temperature T can be written as:

$$x_{ex} = \frac{4\pi}{3}\int_0^t I_o \exp(-E_I/RT)\left[r^{*2} + \int_\tau^t D_o \exp(-E_D/RT)dt'\right]^{3/2} d\tau$$

$$\text{or} \quad x_{ex} = \frac{4\pi}{3} I \int_0^t \left[r^{*2} + D(t-\tau)\right]^{3/2} d\tau \tag{14}$$

And assuming r^* is negligible, dx/dt is obtained as:

$$\frac{dx}{dt} = \exp\left[-\frac{(2E_I + 3E_D)}{5RT}\right][(8\pi/15)I_o]^{\frac{2}{5}} D_0^{\frac{3}{5}} \frac{5}{2}(1-x)[\ln(1-x)]^{3/5}$$

$$\text{or} \quad \frac{dx}{dt} = \frac{5}{2}[(8\pi/15)I]^{\frac{2}{5}} D^{\frac{3}{5}}(1-x)[\ln(1-x)]^{3/5} \tag{15}$$

If Eq. (15) is compared with Eqs. (2a) and (7), analogous results to Eq. (A-3) are obtained:

$$E_a = \frac{2E_I + 3E_D}{5} \quad \text{and} \quad n = 5/2 \tag{16a}$$

$$P_{iso}^{KJMA}(x) = \frac{P_{0,iso}[-\ln(1-x)]^{-\frac{3}{5}}}{\frac{5}{2}(1-x)} \tag{16b}$$

with

$$P_{0,iso}^{-1} = \left[\frac{8\pi}{15} I_o\right]^{\frac{2}{5}} D_o^{\frac{3}{5}} \tag{16c}$$

The Avrami exponent obtained is a characteristic result of a three-dimensional growth controlled by diffusion with constant nucleation rate [14].

2.2. Continuous heating regime

The extended transformation fraction x_{ex}, as a function of time, at continuous heating regime ("HR" is used as subindex) can be written (assuming r^* is negligible) using Eqs. (9a), (10), (11), (12) and (13) (see Appendix B, Eqs. (B-12) and (B-13)):

$$x_{ex} = \frac{8\pi I D^{3/2}}{15\beta^{5/2}}\left[\frac{RT^2}{E_D}\right]^{\frac{5}{2}}\left(\phi_{5/2}(E_I/E_D)\right)^{5/3} \tag{17}$$

with

$$\phi_{5/2}(B) = \left[\frac{5}{2}\sum_{i=0}^{\infty}\binom{3/2}{i}\frac{(-1)^i}{B+i}\right]^{3/5} \tag{18}$$

And the transformation rate dx/dt is obtained using Eqs. (B-22) and (B-23) (See Appendix B):

$$\frac{dx}{dt} = \left[\frac{8\pi}{15}\right]^{\frac{2}{5}} I_o^{2/5} D_o^{3/5} \frac{5}{2}(1-x)(-\ln(1-x))^{3/5} \exp\left(-\frac{2E_I + 3E_D}{5RT}\right)\psi_{5/2}(E_I/E_D)$$

$$\text{or} \quad \frac{dx}{dt} = \frac{5}{2}\left[\frac{8\pi}{15}\right]^{\frac{2}{5}} I^{2/5} D^{3/5}(1-x)(-\ln(1-x))^{3/5}\psi_{5/2}(E_I/E_D) \tag{19}$$

with

$$\psi_{5/2}(B) = \frac{\frac{3}{2}\sum_{i=0}^{\infty}\binom{1/2}{i}\frac{(-1)^i}{B+i}}{\phi_{5/2}(B)} \tag{20}$$

Comparing Eq. (19) with Eqs. (2a) and (7), analogous results to Eqs. (A-3) and (16) are obtained:

$$E_a = \frac{2E_I + 3E_D}{5} \quad \text{and} \quad n = 5/2 \tag{21a}$$

$$P_{HR}^{KJMA}(x) = \frac{P_{0,HR}[-\ln(1-x)]^{-\frac{3}{5}}}{\frac{5}{2}(1-x)}\psi_{5/2}(E_I/E_D) \tag{21b}$$

with

$$P_{0,HR}^{-1} = P_{0,iso}^{-1} = \left[\frac{8\pi}{15} I_o\right]^{\frac{2}{5}} D_o^{\frac{3}{5}} \tag{21c}$$

Using Eq. (16b), Eq. (21b) can be written as:

$$P_{HR}^{KJMA}(x) = P_{iso}^{KJMA}(x)\psi_{5/2}(E_I/E_D) \tag{21d}$$

Based on Eq. (19), under the assumptions of this work, the validity of the additivity rule for diffusion controlled growth processes is demonstrated. In others words, the transformation rate dx/dt is the product of functions that depend on the temperature T and transformed fraction. It is in agreement with previous work [4,6,7,10,11].

The development of x_{ex} and dx/dt for diffusion controlled growth processes under continuous heating conditions reported here in Eqs (17) and (19) is based on the approximation of large activation energy [28,29] and is similar to those in previous works [4,11].

Based on the exact solution of isothermal and non-isothermal diffusion controlled growth, Tomellini [10] demonstrated that the non-isothermal kinetic converges to isothermal kinetic in the limit of zero heating rate and its exact solution is compatible with Eq. (19) in the case of large activation energy.

The new functions $\varphi_{5/2}(B)$ and $\Psi_{5/2}(B)$ are plotted versus $B = E_I/E_D$ in Fig. 1. These functions were determined numerically with a relative error less than 10^{-12}.

It is therefore concluded that diffusion controlled growth of homogeneously nucleating crystalline grains does not pertain to an isokinetic reaction except for $E_I = E_D$ in agreement with previous works [4,6,7,10,11]. However, a novel analysis of the kinetic function is shown here. Considering the Eq. (21d), apart from the factor $\Psi_{5/2}(E_I/E_D)$ a unique function $P(x)$ describes both continuous heating and isothermal transformation rate in the form given by Eqs. (2a) and (2b). Consequently, the coupling of experimental data in both regimes may allow the E_I/E_D ratio to be determined.

The aim of this work is: to perform the master curve analysis (using Eqs. (4a) and (4b)) of the continuous heating calorimetric

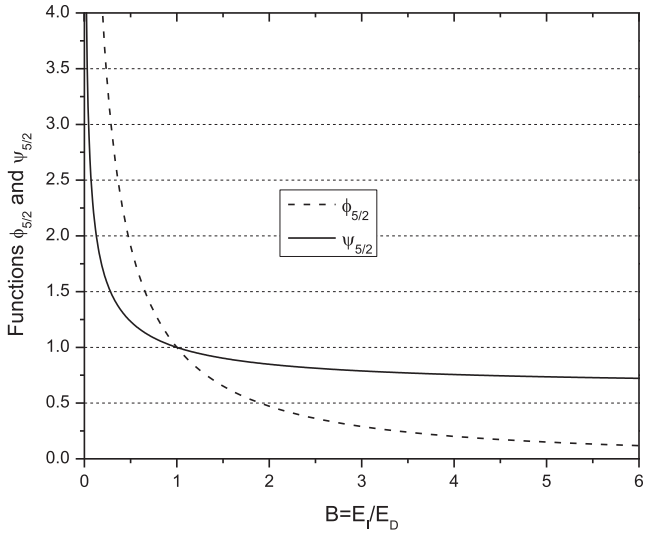

Fig. 1. Functions $\varphi_{5/2}(B)$ and $\Psi_{5/2}(B)$ versus $B = E_I/E_D$ (Eqs. (18) and (20))). If $B = E_I/E_D = 1$, $\varphi_{5/2}(E_I/E_D) = \Psi_{5/2}(E_I/E_D) = 1$ and therefore, diffusion controlled 3D growth of nucleating crystals is an isokinetic reaction.

data obtained for the $(Ge_{0.25}Se_{0.75})_{100-y}Ag_y$ glassy alloys crystallization and to compare the experimental function $P_{HR}(x)$ (Eq. (2b) or (6)) with those obtained with the JMAK model for 3D growth controlled by diffusion (Eqs. (21a–c)).

3. Application to the crystallization of AgGeSe amorphous alloys

3.1. Master curve analysis of the crystallization process

In a previous work [25] glasses with compositions $(Ge_{25}Se_{75})_{100-y}$ Ag_y (with y = 10, 15, 20 and 25 at.%) were synthesized and their thermal evolution heating has been studied by differential scanning calorimetry (DSC) (Continuous heating experiments were performed at scan rates β between 10 and 80 K/min).

Fig. 2 shows the DSC curves obtained in a previous work [25] for the crystallization of $(Ge_{25}Se_{75})_{100-y}$ Ag_y (with y = 10, 15, 20 and 25 at.%) amorphous alloys.

The thermal analysis was carried out in a differential scanning calorimeter Perkin Elmer DSC-7 under dynamic Ar atmosphere. All powder samples weighting 5.00 ± 0.05 mg were sealed in aluminium pans. Continuous heating experiments were performed at scan rates β = 10, 20, 40 and 80 K min^{-1}.

Two main exothermic transformations occur. They correspond to a primary crystallization of the high temperature phase γ-Ag_8GeSe_6 and a secondary crystallization of $GeSe_2$ [25]. The $(Ge_{25}Se_{75})_{75}$ Ag_{25} sample is quite different. It shows a different shape of the glass transition shift and a small exothermic peak (intermediate peak) between the two main peaks.

The master curve method, developed in Section 1.1, was applied to the DSC data of the first crystallization (γ-Ag_8GeSe_6 phase) obtained in the continuous heating mode. Fig. 3 shows the transformation rate dx/dT obtained from DSC data at 10, 20, 40 and 80 K/min for all the samples. The average master curve at 40 K/min was determined with the best overlapping of the experimental data in the master curve (Eqs. (4a) and (4b)) and its value E_a are shown in Table 1 (fitting coefficient $\chi^2 \sim 10^{-7}$). The initial estimates of E_a [25], obtained by the Kissinger method [16], is shown in Table 1 and they are in good agreement except for y = 25. The results show that the

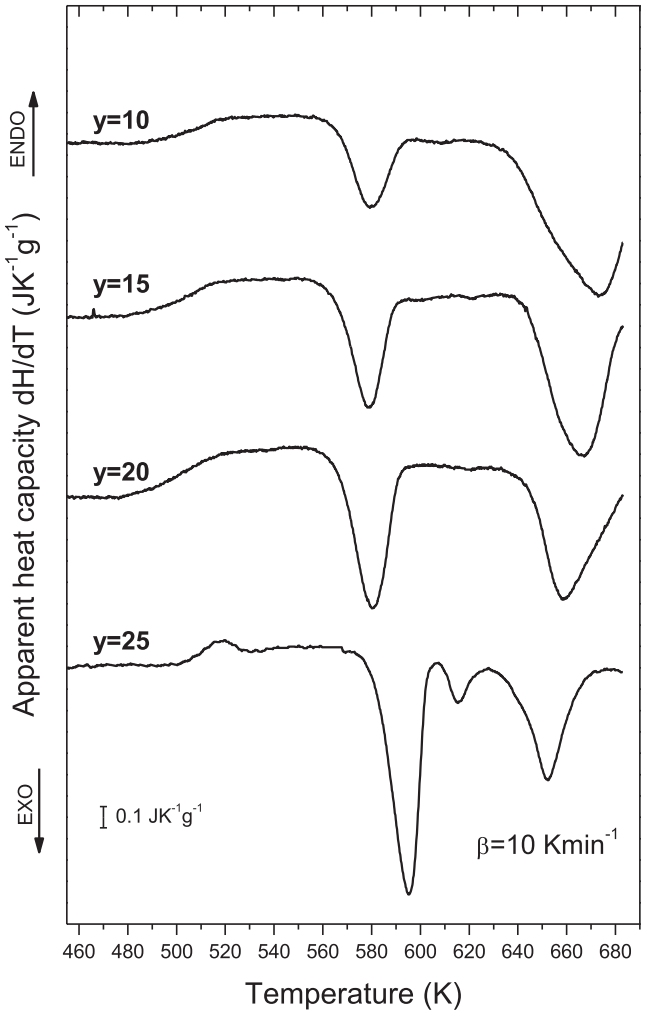

Fig. 2. DSC curves (dH/dT versus T, where H is the enthalpy in J/g and T the temperature in K) obtained during the crystallization of glasses $(Ge_{25}Se_{75})_{100-y}$ Ag_y (with y = 10, 15, 20 and 25 at.%) at a heating rate of 10 K/min [25].

activation energy is quite similar in all the analysed compositions (close to 2.25 eV/at) observing a small increase with the Ag content. Such similarity in the E_a values is expected on considering that: (i) at high undercooling the temperature dependence of crystallization is dominated by the viscosity of the metastable liquid alloy and (ii) the apparent activation energy of the viscosity has a soft composition dependence [25].

The individual calculated curves at the equivalent heating rate $\beta_{eq} = 40$ K/min, obtained from the experimental DSC data, and the master curve are shown in Fig. 3. The good agreement in between the different calculated curves confirms the validity of the master curve method to analyse the continuous heating primary crystallization process of the glasses $(Ge_{25}Se_{75})_{100-y}$ Ag_y (y = 10, 15, 20 and 25 at.%) and gives a confident value of their respective apparent activation energy.

3.2. Analysis of the kinetic mechanisms involved in the crystallization process

Once the master curve has been calculated, the $P_{HR}(x)$ kinetic function can be determined by applying Eq. (6) to the master curve in order to study the kinetics of the primary crystallization. These $P_{HR}(x)$ "experimental" data, obtained using Eq. (6), are shown in

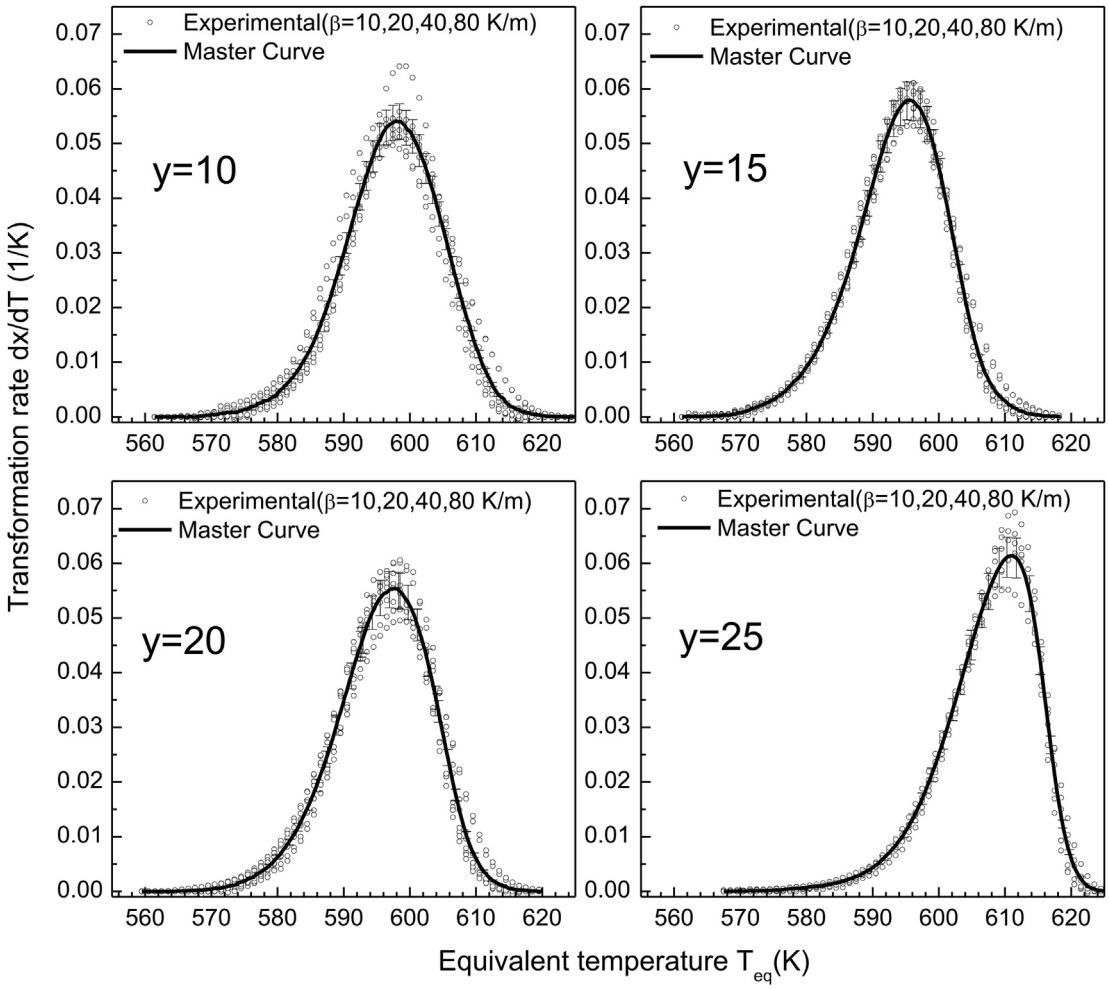

Fig. 3. The transformation rate *dx/dT* vs. the equivalent temperature T_{eq} calculated from experimental data by use of Eq. (4b) obtained for the crystallization of glasses $(Ge_{25}Se_{75})_{100-y}$ Ag_y (with y = 10, 15, 20 and 25 at.%) at 10, 20, 40 and 80 K/min and the corresponding *master curve* (see Section 1.1). Some error bars are shown.

Table 1
The activation energy E_a obtained with the master curve procedure, showed in Section 1.1 (coefficient of the fit $\chi^2 = 10^{-7}$), the activation energy E_a obtained by Kissinger method [16], the Avrami exponent at the transformation begin n_{begin} and at the transformation end n_{end}, the time constant at the transformation begin $Po^{-1}{}_{begin}$ [Range of fits: 0.01 < x < 0.03 (transformation begin) and 0.96 < x < 0.99 (transformation end), the correlation coefficients are about 0.999 (begin) and 0.98 (end)] for the crystallization of the phase γ-Ag_8GeSe_6 in glasses $(Ge_{25}Se_{75})_{100-y}$ Ag_y (with y = 10, 15, 20 and 25 at.%) *Simulated parameters*: the time constant simulated P_o^{-1} was determined using Eq. (16c), γ is the crystallized fraction at the end of the primary crystallization (x = 1).

y		10	15	20	25
E_a (eV/at) Master curve		2.04 ± 0.03	2.23 ± 0.03	2.20 ± 0.03	2.58 ± 0.03
E_a (eV/at) Kissinger [16]		2.04 ± 0.10	2.24 ± 0.10	2.09 ± 0.10	2.32 ± 0.10
n_{begin}		2.50 ± 0.01	2.48 ± 0.01	2.31 ± 0.01	2.15 ± 0.01
n_{end}		0.64 ± 0.02	0.70 ± 0.02	0.89 ± 0.02	1.33 ± 0.02
$Po^{-1}{}_{begin}$ (s^{-1}) (experimental)		$(6.8 \pm 0.4)10^{15}$	$(4.9 \pm 0.3)10^{17}$	$(2.1 \pm 0.1)10^{17}$	$(1.1 \pm 0.1)10^{20}$
Simulated	Po^{-1} (s^{-1}) ± 0.03 10^{15}	$6.81 \cdot 10^{15}$	$4.65 \cdot 10^{17}$	$2.22 \cdot 10^{17}$	$1.42 \cdot 10^{20}$
	γ ± 0.01	0.50	0.50	0.50	0.50

Fig. 4.

Based on Eq. (21d), in the KJMA model, the kinetic functions $P_{HR}(x)$ and $P_{iso}(x)$ in both continuous heating and isothermal transformations are the same except for the factor $\psi_{5/2}(E_I/E_D)$. Consequently, $log(P_{HR}(x)) = log(P_{iso}(x)) + C$ with C a factor which depends on the nucleation and diffusion activation energies ratio. Therefore, assuming constant the nucleation and diffusion activation energies ratio, the functional dependence of $P(x)$ on x is the same under both continuous heating and isothermal conditions.

With the aim to compare the "experimental" $P_{HR}(x)$ function and the $P_{iso}^{KJMA}(x)$ one described in the JMAK theory for nucleation/growth, the asymptotic behaviour at the beginning (transformed fraction 0.01 < x < 0.03) and at the end (transformed fraction 0.96 < x < 0.99) of the transformation were fitted to Eq. (7) with fixed values of the Avrami exponent. The parameters (n and P_o^{-1}), used for the asymptotic fittings at the beginning (n_{begin} and $P_o^{-1}{}_{begin}$) and the end (n_{end}) of the transformation, are shown in Table 1. These parameters indicate that the initial stages of the primary crystallization can be described within the KJMA model with, depending of the Ag content y, a kinetic exponent n about 2.1–2.5

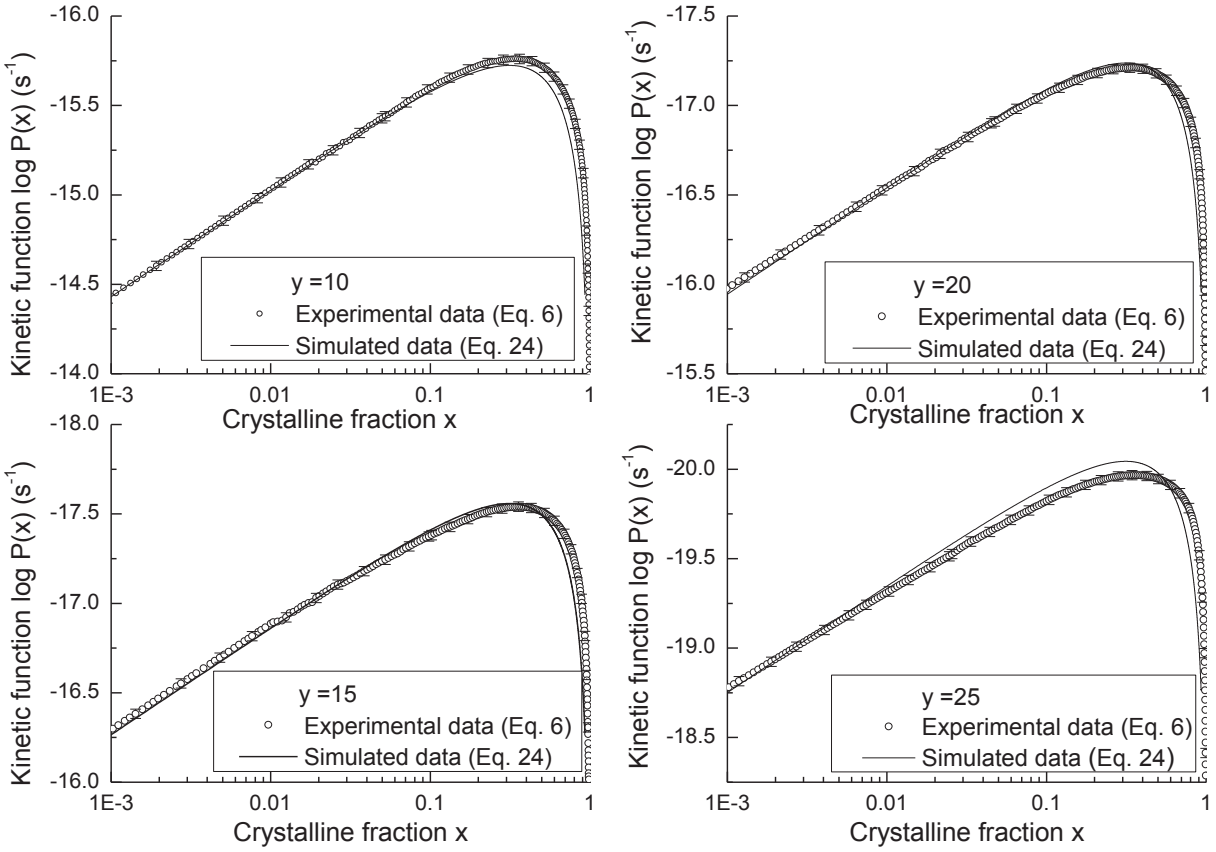

Fig. 4. The kinetic function $P(x)$ for the crystallization of the γ-Ag_8GeSe_6 phase in glasses $(Ge_{25}Se_{75})_{100-y}$ Ag_y (with y = 10, 15, 20 and 25 at.%) obtained from: a) Experimental data $P_{HR}(x)$ (using Eq. (6) and the master curve) –symbols-; b) Simulated data $P_{soft}(x)$ from a model diffusion-controlled-3D growth with decreasing homogeneous nucleation and soft impingement (Eq. (24)) –full line-. Some error bars are shown.

(see Table 1). Although the interpretation of this coefficient is not straightforward, these values of n lie between 3/2 (diffusion-controlled growth of pre-existing grains) and 5/2 (diffusion-controlled growth with constant nucleation rate, see Section 2 and Eqs. (A-3a) and (16a)) [21,22]. These values of n can also be identified with a decreasing nucleation rate combined with diffusion controlled grain growth (for $3/2 < n < 5/2$) [9,12,14,21–23,26]. On the other hand, the decrease of the slope in the log-log graphic $P_{HR}(x)$ vs. x (see Fig. 4) shows that the kinetic exponent n decreases monotonously with the crystallization fraction x (see Eq. (7)) [21,22,27]. Therefore, the values of n_{end} (see Table 1) and the analysis of the whole crystallization process, where n decreases monotonously, let us to conclude that the best hypothesis of the crystallization kinetic is diffusion-controlled-3D growth combined with a decreasing nucleation rate [2,12,21–23]. Consequently, the model shown in Section 2 has been extended by modifying Eqs. (9a) and (13) to include a decreasing nucleation rate, I_{soft}, and a diffusion controlled-3D growth with soft impingement – diffusion coefficient D_{soft}–. The forms of I_{soft} and D_{soft} are:

$$I_{soft} = I(T)\frac{(1-x)^2}{(1-\gamma x)^2} \tag{22a}$$

$$D_{soft} = D(T)\frac{(1-x)}{(1-\gamma x)} \tag{22b}$$

where $I(T)$ and $D(T)$ are given by Eqs. (9a) and (13), γ is the crystallized fraction at the end of the primary crystallization ($x = 1$). Although a nucleation lineal dependence on the factor $(1-x)/(1-\gamma x)$ is commonly proposed in soft impingement [2,12,21,22], based on a previous work [23], a quadratic dependence is used in this work. In this case, the fitting of the kinetic function P(x) shown in Fig. 4 is more suitable.

Therefore, the extended transformation fraction x_{ex} can be written as [9,21,22,27]:

$$x_{ex}(t) = \frac{4\pi}{3}\int_0^t I_{soft}(\tau)\left[\int_\tau^t D_{soft}(t')dt'\right]^{3/2} d\tau$$
$$= \frac{4\pi}{3}\int_0^t I(T)\frac{(1-x(\tau))^2}{(1-\gamma x(\tau))^2}\left[\int_\tau^t D(T)\frac{(1-x(t'))}{(1-\gamma x(t'))}dt'\right]^{3/2} d\tau \tag{23}$$

where $x_{ex}(t)$, is related to $x(t)$ by Eq. (10):

$$x(t) = 1 - \exp(-x_{ex}(t))$$

These Eqs. (23) and (10) are an integral-differential equations system (where the crystallized fraction $x(t)$ is the unknown function) and were solved numerically. For a fixed time t_n, the procedure is an iterative method, where the fraction transformed is re-estimated at every step of the iteration process. The iteration procedure starts with an initial value of x corresponding to the previous instant t_{n-1}, and $x(t_n)$ is re-calculated using Eqs. (23) and (10) iteratively until the convergence, with an accuracy of 10^{-8} in x.

The parameters of the simulated curves are shown in Table 1. These equations reproduce qualitatively the continuous decay of both nucleation frequency (due to the decrease of supersaturation of the disordered matrix) and the concentration gradient ahead of the interface (due to soft impingement between grains).

The validity of this complex model of diffusion-controlled-3D growth with decreasing homogeneous nucleation and soft impingement was explored by determining the kinetic function $P_{soft}(x)$. This function was calculated from the simulated curves of the transformation rate, $\left.\frac{dx}{dt}\right|_{soft}$, using Eq. (2a). Namely,

$$P_{soft}(x) = \frac{\exp\left(\frac{-E_a}{kT}\right)}{\left.\frac{dx}{dt}\right|_{soft}} \tag{24}$$

The results are shown in Fig. 4. The simulated values of $P_{soft}(x)$ show good agreement with the experimental curves $P_{HR}(x)$ obtained using the master curve procedure and Eq. (6). This model reproduces acceptably the whole crystallization process except for y = 25%. This fact can be explained with the small exothermic peak (intermediate peak) between the two main peaks observed in Fig. 2 for the $(Ge_{25}Se_{75})_{75}$ Ag_{25} sample. It is possible that the overlapping of the intermediate peak with the primary transformation affects the baseline.

Also, the experimental value of ${P_o^{-1}}_{begin}$ is close to the simulated one (see Table 1).

The Avrami exponent of the studied samples decreases with x and has very low values at the end of the crystallization. This behaviour can be explained by analysing the morphology of the $(Ge_{25}Se_{75})_{100-y}$ Ag_y amorphous samples. As a consequence of the liquid miscibility gap, $(Ge_xSe_{100-x})_{100-y}$ Ag_y bulk glasses (x = 20, 25 at.% and 5 < y < 25 at.%) are inhomogeneous with two amorphous phases, one with higher Ag content and other with lower Ag concentration [30–32]. The size of these phases depends on the composition ranging from 100 nm to a few microns. The primary crystallization of the γ-Ag_8GeSe_6 phase occurs preferably in the amorphous phase rich in silver. Based on the crystal composition, the nucleus of γ-Ag_8GeSe_6 are originated with greater probability in zones rich in Ag and grow affected by the composition change of the remaining phase. The growth decreases dramatically at the edge of the poor silver zone.

4. Conclusions

Diffusion controlled growth of homogeneously nucleating crystalline grains does not pertain to an isokinetic reaction except for $E_I = E_D$. However, considering the Eq. (21d), apart from the factor $\Psi_{5/2}(E_I/E_D)$ a unique function $P(x)$ describes both continuous heating and isothermal transformation rate. Therefore, the coupling of experimental data in both regimes may allow the E_I/E_D ratio to be determined.

The master curve method has been applied to perform the kinetic analysis of the continuous heating calorimetric data. It is shown that the primary crystallization process of the glasses $(Ge_{25}Se_{75})_{100-y}$ Ag_y (y = 10, 15, 20 and 25 at.%) may be described by a unique function $P_{HR}(x)$ on varying heating rate. The master curve was computed using continuous heating experimental data without crystallization model information. In other words, the master curve is the "average" of the experimental data. The values of apparent activation energy, obtained for the primary crystallization of the phase γ-Ag_8GeSe_6, are in the range: 2.0 eV/at < E_a < 2.6 eV/at. The apparent activation energy increases when the Ag content increases.

The primary crystallization growth of the phase γ-Ag_8GeSe_6, is controlled by diffusion. A model of the decrease of both nucleation rate and effective diffusion in primary crystallization, such as the one described above, is able to reduce the Avrami exponent at the onset of the transformation, from the *ideal* value of 5/2 to values close to those observed experimentally (2.1 < n < 2.5).

In the final stages of crystallization (0.96 < x < 0.99), the experimental kinetic function $P_{HR}(x)$ may be approached by an Avrami function with an exponent n in the range 0.6–1.3. Values of this parameter about or smaller than the unity have been previously related to soft impingement processes [12,21,22], where grain growth is kinetically slowed down, and eventually inhibited, by the change of concentration in the untransformed region. This behaviour can be associated with the inhomogeneity of the glasses.

Conflict of interest

The authors declare that they have no conflict of interest.

Acknowledgments

This study was funded by the project number 20020100100468 (Consejo Nacional de Investigaciones Científicas y Técnicas – CONICET) and the project number 20020130100647BA (Universidad de Buenos Aires).

Appendix A. Johnson-Mehl-Avrami-Kolmogorov theory. Growth controlled by interface

In a previous work [23], a KJMA model with homogenous and constant nucleation and three-dimensional interface-controlled growth was elaborated under isothermal and continuous heating regimes, using the following hypothesis:

a) The nucleation critical radius is negligible.
b) An Arrhenian temperature dependence for both nucleation frequency I(T) and growth rate u(T), that is:

$$I(T) = I_o \exp\left(\frac{-E_I}{kT}\right) \tag{A-1}$$

$$u(T) = u_o \exp\left(\frac{-E_U}{kT}\right) \tag{A-2}$$

where E_I, and E_U are the activation energies for nucleation and growth, respectively, and I_o and u_o the pre-exponential factors.

It was found [23] under isothermal regime, that the activation energy, the Avrami exponent and the kinetic function $P_{iso}(x)$ in Eq. (2a), are

$$E_a = \frac{E_I + 3E_U}{4} \quad \text{and} \quad n = 4 \tag{A-3a}$$

$$P_{iso}^{KJMA}(x) = \frac{P_{0,iso}[-\ln(1-x)]^{\frac{-3}{4}}}{4(1-x)} \tag{A-3b}$$

with

$$P_{0,iso}^{-1} = \left[\left(\frac{\pi}{3}\right) I_o u_o^3\right]^{\frac{1}{4}} \tag{A-3c}$$

Using the same hypothesis, under continuous heating regimes, in Eq. (2b), the activation energy, the Avrami exponent and the kinetic function$P_{HR}(x)$, are

$$E_a = \frac{E_I + 3E_U}{4} \quad \text{and} \quad n = 4 \tag{A-4a}$$

$$P_{HR}^{KJMA}(x) = \frac{P_{0,HR}[-\ln(1-x)]^{\frac{-3}{4}}}{4(1-x)}\psi_4\left(\frac{E_I}{E_U}\right) \tag{A-4b}$$

with

$$P_{0,HR}^{-1} = P_{0,iso}^{-1} = \left[\left(\frac{\pi}{3}\right)I_o u_o^3\right]^{\frac{1}{4}} \tag{A-4c}$$

and

$$\psi_4(B) = \left[\frac{(3+B)^3 3\left(1 - \frac{2B}{1+B} + \frac{B}{2+B}\right)}{4^3 B}\right]^{1/4} \quad with\ B = \frac{E_I}{E_U} \tag{A-5}$$

Thus Eq. (A-4b) can be written as:

$$P_{HR}^{KJMA}(x) = P_{iso}^{KJMA}(x)\psi_4\left(\frac{E_I}{E_U}\right) \tag{A-6}$$

Based on Eq. (A-6), $P_{iso}(x)$ and $P_{HR}(x)$ are the same function except for the factor ψ_4.

The factor $\psi_4(E_I/E_U)$ is a function of the activation energies ratio E_I/E_U, with an interesting particular case: when $E_I = E_U$, that is $B = 1$, ψ_4 is equal to 1 in only this situation. Thus, it is therefore concluded that the homogenous and constant nucleation and dimensional interface-controlled growth regime behaves as an isokinetic reactions when $E_I = E_U$. In other words, Eq. (A-6) clearly indicates, in general, that the process is non-isokinetic.

Appendix B. Johnson-Mehl-Avrami-Kolmogorov theory. Growth controlled by diffusion

Assuming r^* is negligible, Eq. (14) can be written (with $T = T_o + \beta t$) as:

$$x_{ex} = \frac{4\pi}{3}\int_0^T I_o \exp(-E_I/RT')\left[\int_{T'}^{T} D_o \exp\left(-E_D/RT''\right)dT''/\beta\right]^{3/2} dT'/\beta \tag{B-1}$$

If $E/RT \geq 20$, to compute the integral, we know that [4]:

$$\int_0^T \exp\left(-E/RT''\right)dT'' \cong \frac{RT^2}{E}\exp(-E/RT) \tag{B-2}$$

Eq. (B-2) can be written as:

$$\frac{\partial}{\partial T}\left[\frac{RT^2}{E}\exp(-E/RT)\right] \cong \exp(-E/RT) \tag{B-3}$$

Equivalently [4]:

$$\int_{T'}^{T} \exp\left(-E/RT''\right)dT'' \cong \frac{RT^2}{E}\exp(-E/RT) - \frac{RT'^2}{E}\exp(-E/RT') \tag{B-4}$$

Eq. (B-4) is the approximation of large activation energy, $E/RT >> 1$, of the so called temperature integral [4,8,11]. Other authors [4,8,11] employed the same approximation in the computation of the transformed fraction. The evaluation of the different approximations to the temperature integral was studied by Órfão in a review [29]. On the other hand, the temperature integral was computed exactly by Tomellini [7,10].

Consequently using (B-4) in (B-1):

$$x_{ex} = \frac{4\pi I_o D_o^{3/2}}{3\beta^{5/2}}\left(\left(RT^2/E_D\right)\exp(-E_D/RT)\right)^{3/2} \times \int_0^T \exp(-E_I/RT')(1-\Theta)^{3/2}dT' \tag{B-5}$$

$$\text{with } \Theta = \frac{T'^2\exp(-E_D/RT')}{T^2\exp(-E_D/RT)} \tag{B-6}$$

In Eq. (B-1), $0 < T' <= T$, and $exp(-E_D/RT') <= exp(-E_D/RT) < 1$, therefore $0 < \Theta <= 1$ and the function $[1-\Theta]^{3/2}$ is replaced by its Taylor serie:

$$[1-\Theta]^{3/2} = 1 - 3/2\,\Theta + 3/2\,(3/2-1)\frac{\Theta^2}{2!} - 3/2\,(3/2-1) \times (3/2-2)\frac{\Theta^3}{3!} + \ldots\ldots$$

$$= [1-\Theta]^{3/2} = \sum_{i=0}^{\infty}\binom{3/2}{i}(-1)^i\Theta^i \tag{B-7}$$

$$\text{with } \binom{3/2}{i} = \frac{\prod_{j=0}^{i-1}(3/2-j)}{i!} \text{ if } i \neq 0 \text{ and } \binom{3/2}{0} = 1$$

Substituting into Eq. (B-5):

$$x_{ex} = \frac{4\pi I_o D_o^{3/2}}{3\beta^{5/2}}\left(\left(RT^2/E_D\right)\exp(-E_D/RT)\right)^{3/2}\sum_{i=0}^{\infty}\binom{3/2}{i}(-1)^i \times \int_0^T \exp(-E_I/RT')\Theta^n dT' \tag{B-8}$$

Replacing (B-6) into (B-8):

$$x_{ex} = \frac{4\pi I_o D_o^{3/2}}{3\beta^{5/2}}\left(\frac{RT^2}{E_D}\exp(-E_D/RT)\right)^{3/2} \cdot \sum_{i=0}^{\infty}\binom{3/2}{i}(-1)^i\frac{\exp(nE_D/RT)}{T^{2i}}\int_0^T \exp\left(-(E_I+nE_D)/RT'\right)T'^{2i}dT' \tag{B-9}$$

Using the approximation equivalent to (B-2) [4]:

$$\int_0^T T'^q \exp(-E/RT')dT' \cong \frac{RT^{q+2}}{E}\exp(-E/RT) \tag{B-10}$$

For $q = 0,2,4,6,8$ …. (if $E/RT > 20$)

$$So, \quad x_{ex} = \frac{4\pi I_o D_o^{3/2}}{3\beta^{5/2}}\left(RT^2/E_D\right)^{5/2}\exp\left(-\frac{E_I + 3/2E_D}{RT}\right) \times \sum_{i=0}^{\infty}\binom{3/2}{i}\frac{(-1)^i E_D}{E_I + iE_D} \tag{B-11}$$

Eq. (B-11) can be written as:

$$Or,\ \ x_{ex} = \frac{8\pi I D^{3/2}}{15\beta^{5/2}}\left(RT^2/E_D\right)^{5/2}\left(\phi_{5/2}(E_I/E_D)\right)^{5/3} \tag{B-12}$$

with

$$\phi_{5/2}(B) = \left[\frac{5}{2}\sum_{i=0}^{\infty}\binom{3/2}{i}\frac{(-1)^i}{B+i}\right]^{3/5} \tag{B-13}$$

With the same hypothesis, the time derivative dx_{ex}/dt is obtained using (B-5):

$$\begin{aligned}\frac{dx_{ex}}{dt} &= \beta\frac{dx_{ex}}{dT}\\ &= \frac{4\pi I_o D_o^{3/2}}{3\beta^{3/2}}\frac{\partial}{\partial T}\left[\left(RT^2/E_D\right)^{3/2}\exp\left(\frac{-3E_D}{2RT}\right)\right.\\ &\quad\left.\times\int_0^T\exp\left(\frac{-E_I}{RT'}\right)[1-\Theta]^{3/2}dT'\right]\end{aligned} \tag{B-14}$$

In (B-14), using $E_D/RT >> 1$:

$$\begin{aligned}\frac{\partial}{\partial T}\left[\left(RT^2/E_D\right)^{3/2}\exp\left(\frac{-3E_D}{2RT}\right)\right] &= \frac{3}{2}\left[\left(RT^2/E_D\right)^{1/2}\right.\\ &\quad\left.\times\exp\left(\frac{-3E_D}{2RT}\right)\right]\left(\frac{2RT}{E_D}+1\right)\\ &\approx\frac{3}{2}\left(\left(RT^2/E_D\right)\exp\left(\frac{-E_D}{RT}\right)\right)^{1/2}\\ &\quad\times\exp\left(\frac{-E_D}{RT}\right)\end{aligned} \tag{B-15}$$

And using $\frac{\partial\Theta}{\partial T} = -\frac{\Theta}{T}\left(2+\frac{E_D}{RT}\right)\approx -\Theta\frac{E_D}{RT^2}$:

$$\begin{aligned}&\frac{\partial}{\partial T}\left[\int_0^T\exp\left(\frac{-E_I}{RT'}\right)[1-\Theta]^{3/2}dT'\right]\\ &= \int_0^T\exp\left(\frac{-E_I}{RT'}\right)\frac{\partial}{\partial T}[1-\Theta]^{3/2}dT'\\ &= \int_0^T\exp\left(\frac{-E_I}{RT'}\right)\frac{3}{2}[1-\Theta]^{1/2}(-1)\frac{\partial\Theta}{\partial T}dT'\\ &= \int_0^T\exp\left(\frac{-E_I}{RT'}\right)\frac{3}{2}[1-\Theta]^{1/2}\Theta\frac{E_D}{RT^2}dT'\end{aligned} \tag{B-16}$$

Therefore, (B-14) can be written as:

$$\begin{aligned}\frac{dx_{ex}}{dt} &= \frac{2\pi I_o D_o^{3/2}}{\beta^{3/2}}\left(\left(RT^2/E_D\right)\right)^{1/2}\exp\left(\frac{-3E_D}{2RT}\right)\int_0^T\exp\left(\frac{-E_I}{RT'}\right)\\ &\quad\times\left\{[1-\Theta]^{3/2}+\Theta[1-\Theta]^{1/2}\right\}dT'\end{aligned}$$

$$\begin{aligned}\frac{dx_{ex}}{dt} &= \frac{2\pi I_o D_o^{3/2}}{\beta^{3/2}}\left(\frac{RT^2}{E_D}\exp\left(\frac{-E_D}{RT}\right)\right)^{1/2}\exp\left(\frac{-E_D}{RT}\right)\\ &\quad\times\int_0^T\exp\left(\frac{-E_I}{RT'}\right)[1-\Theta]^{1/2}dT'\end{aligned} \tag{B-17}$$

As it was mentioned before, $0 < \Theta <= 1$ and the function $[1-\Theta]^{1/2}$ is replaced by its Taylor serie:

$$[1-\Theta]^{1/2} = \sum_{i=0}^{\infty}\binom{1/2}{i}(-1)^i\Theta^i \tag{B-18}$$

with $\binom{1/2}{i} = \frac{\prod_{j=0}^{i-1}(1/2-j)}{i!}$ if $i\neq 0$ and $\binom{1/2}{0} = 1$

Similarity, as it was done in Eqs. (B-5), (B-8) and (B-9), the integral in Eq. (B-17) can be written, using the approximation (B-10):

$$\begin{aligned}\int_0^T\exp\left(\frac{-E_I}{RT'}\right)[1-\Theta]^{1/2}dT' &= \sum_{i=0}^{\infty}\binom{1/2}{i}(-1)^i\frac{\exp(nE_D/RT)}{T^{2i}}\\ &\quad\times\int_0^T\exp(-(E_I+nE_D)/RT')T'^{2i}dT'\\ &= RT^2\exp(-(E_I)/RT)\sum_{i=0}^{\infty}\binom{1/2}{i}\frac{(-1)^i}{E_I+iE_D}\end{aligned} \tag{B-19}$$

Therefore, substituting into Eq. (B-17):

$$\begin{aligned}\frac{dx_{ex}}{dt} &= \frac{2\pi I_o D_o^{3/2}}{\beta^{3/2}}\left(RT^2/E_D\right)^{3/2}\exp\left(-\frac{E_I+3/2E_D}{RT}\right)\\ &\quad\times\sum_{i=0}^{\infty}\binom{1/2}{i}\frac{(-1)^iE_D}{E_I+iE_D}\end{aligned}$$

$$\text{Or}\quad \frac{dx_{ex}}{dt} = \frac{2\pi I D^{3/2}}{\beta^{3/2}}\left(RT^2/E_D\right)^{3/2}\sum_{i=0}^{\infty}\binom{1/2}{i}\frac{(-1)^i}{E_I/E_D+i} \tag{B-20}$$

But, using Eqs. (B-11) and (B-12):

$$\begin{aligned}(x_{ex})^{3/5} &= \left(8\pi I_o D_0^{3/2}/15\beta^{5/2}\right)^{3/5}\left(RT^2/E_D\right)^{3/2}\\ &\quad\times\left(\exp\left(-\frac{2E_I+3E_D}{2RT}\right)\right)^{3/5}\phi_{5/2}(E_I/E_D)\end{aligned}$$

$$\text{Or}\quad (x_{ex})^{3/5} = \left(8\pi I D^{3/2}/15\beta^{5/2}\right)^{3/5}\left(RT^2/E_D\right)^{3/2}\phi_{5/2}(E_I/E_D) \tag{B-21}$$

Eq. (B-20) can be written:

$$\frac{dx_{ex}}{dt} = (8\pi/15)^{2/5}I_o^{2/5}D_o^{3/5}\frac{5}{2}(x_{ex})^{3/5}\exp\left(\frac{-2E_I+3E_D}{5RT}\right)\psi_{5/2}(E_I/E_D)$$

$$\text{Or}\quad \frac{dx_{ex}}{dt} = \frac{5}{2}(8\pi/15)^{2/5}I^{2/5}D^{3/5}(x_{ex})^{3/5}\cdot\psi_{5/2}(E_I/E_D) \tag{B-22}$$

With

$$\psi_{5/2}(B) = \frac{\frac{3}{2}\sum_{i=0}^{\infty}\binom{1/2}{i}\frac{(-1)^i}{B+i}}{\phi_{5/2}(B)} \tag{B-23}$$

References

[1] Zhou D, Grant DJW. Model dependence of the activation energy derived from non isothermal kinetic data. J Phys Chem A 2004;108:4239–46.
[2] Liu F, Sommer F, Bos C, Mittemeijer EJ. Analysis of solid state phase transformation kinetics: models and recipes. Int Mater Rev 2007;52(4):193–212.
[3] Vazquez J, Barreda DGG, Lopez-Alemany PL, Villares P, Jimenez-Garay R. A study on non-isothermal transformation kinetics. Application to the crystallization of the Ge0.18Sb0.23Se0.59 glassy alloy. Mater Chem Phys 2006;96:107–15.
[4] Vazquez J, Wagner C, Villares P, Jiménez-Garay R. A theoretical method for determining the crystallized fraction and kinetic parameters by DSC, using non-isothermal techniques. Acta Mater 1996;44:4807–13.
[5] Mittemeijer. Review. Analysis of the kinetics of phase transformations. J Mater Sci 1992;27:3977.
[6] Song SJ, Liu F, Jiang YH. Generalized additivity rule and isokinetics in diffusion-controlled growth. J Mater Sci 2014;49:2624.
[7] Tomellini M. Generalized additivity rule for the Kolmogorov–Johnson-Mehl-Avrami kinetics. J Mater Sci 2015;50:4516.
[8] Farjas J, Roura P. Modification of the Kolmogorov–Johnson–Mehl–Avrami rate equation for non-isothermal experiments and its analytical solution. Acta Mater 2006;54:5573–9.
[9] Fontana M, Arcondo B, Clavaguera-Mora MT, Clavaguera N. Crystallization kinetics driven by two simultaneous modes of crystal growth. Philos Mag B 2000;80(10):1833–56.
[10] Tomellini M. Kolmogorov–Johnson–Mehl–Avrami kinetics for non-isothermal phase transformations ruled by diffusional growth. J Therm Anal Calorim 2014;116:853.
[11] Ruitenberg G, Woldt E, Petford-Long AK. Comparing the Johnson–Mehl–Avrami–Kolmogorov equations for isothermal and linear heating conditions. Thermochim Acta 2001;378:97–105.
[12] Clavaguera-Mora MT, Clavaguera N, Crespo D, Pradell T. Crystallisation kinetics and microstructure development in metallic systems. Prog Mater Sci. 2002;47(6):559–619.
[13] Blazquez JS, Conde CF, Conde A. Non-isothermal approach to isokinetic crystallization processes: application to the nanocrystallization of HITPERM alloys. Acta Mater 2005;53:2305–11.
[14] Christian JW. The theory of phase transformations in Metals and alloys. Oxford: Pergamon Press; 2002.
[15] Cahn JW. Transformation kinetics during continuous cooling. Acta Metall 1956;4:572–5.
[16] Kissinger HE. Reaction kinetics in differential thermal analysis. Anal Chem 1957;29:1702–6.
[17] Avrami M. Kinetics of phase change I. General theory. J Chem Phys 1939;7:1103–12.
[17a] Avrami M. Kinetics of phase change II. Transformation-time relations for random distribution of nuclei. J Chem Phys. 1940;8:212–24.
[18] Avrami M. Granulation, phase change, and microstructure kinetics of phase change. III. J Chem Phys. 1941;9:177–84.
[19] Johnson WA, Mehl RF. Reaction kinetics in processes of nucleation and growth. Trans Am Inst Min Metall Eng 1939;135:416–42.
[20] Kolmogorov AN. On the statistical theory of the crystallization of metals. Bull Acad Sci USSR, Math Ser 1937;1:355–9.
[21] Jacovkis D, Xiao Y, Rodriguez-Viejo J, Clavaguera-Mora M:T:, Clavaguera N. Mechanisms driving primary crystallization of Al87Ni7Cu 3Nd 3 amorphous alloy. Acta Mater 2004;52(9):2819–26.
[22] Jacovkis D, Rodriguez-Viejo J, Clavaguera-Mora MT. Isokinetic analysis of nanocrystallization in an Al–Nd–Ni amorphous alloy. J Phys Condens Matter 2005;17(32):4897.
[23] Fontana M, Arcondo B, Clavaguera-Mora MT, Clavaguera N. Mechanisms controlling primary crystallisation of Ga20Te80 glasses. J Non-Cryst solids 2007;353(22):2131–42.
[24] Torrens-Serra J, Bruna P, Stoica M, Roth S, Eckert J. Glass forming ability, thermal stability, crystallization and magnetic properties of [(Fe,Co,Ni)0.75 Si0.05 B0.20]95 Nb4 Zr1 metallic glasses. J Non-Cryst Solids 2013;367:30–6.
[25] Ureña MA, Fontana M, Arcondo B, Clavaguera-Mora MT. Crystallization processes of Ag–Ge–Se superionic glasses. J Non-Cryst solids 2003;320(1):151–67.
[26] Clavaguera-Mora MT. Glassy materials: thermodynamic and kinetic quantities. J Alloys Compd 1995;220(1):197–205.
[27] Clavaguera N, Clavaguera-Mora MT, Fontana M. Accuracy in the experimental calorimetric study of the crystallization kinetics and predictive transformation diagrams: application to a Ga-Te amorphous alloy. J Mater Res 1998;13(3):744–53.
[28] Starink MJ. The determination of activation energy from linear heating rate experiments: a comparison of the accuracy of iso-conversion methods. Thermochim Acta 2003;404:163.
[29] Orfao Jose JM. Review and evaluation of the approximations to the temperature integral. AIChE J 2007;53:2905.
[30] Ureña MA, Fontana M, Piarristeguy A, Arcondo B. AgGeSe-based bulk glasses: a survey of their fundamental properties. J Alloys Compd 2010;495:305.
[31] Arcondo B, Ureña MA, Piarristeguy A, Pradel A, Fontana M. Nanoscale intrinsic heterogeneities in Ag-Ge-Se glasses and their correlation with physical properties. Appl Surf Sci 2007;254:321.
[32] Wang Y, Mitkova M, Georgiev DG, Mamedov S, Boolchand P. Macroscopic phase separation of Se-rich (x< 1/3) ternary Agy(GexSe1−x)1−y glasses. J Phys Condens Matter 2003;15:S1573.